Effect of delamination on the high frequency wave dispersion of composite beams with active piezosensors

Chrysochoidis, Nikolaos A. ; Anyfantis, Konstantinos; Saravanos, Dimitris A.

Published in:
Proceedings of COMP07: 6th International Symposium on Advanced Composites

Publication date:
2007

Document Version
Publisher's PDF, also known as Version of record

Proceedings of COMP07:
6th International Symposium on Advanced Composites
16-18 May, 2007, Corfu, Greece

COMP2007-094

EFFECT OF DELAMINATION ON THE HIGH FREQUENCY WAVE DISPERSION OF COMPOSITE BEAMS WITH ACTIVE PIEZOSENSORS

Nikolaos A. Chrysochoidis, Konstantinos N. Anyfantis and Dimitris A. Saravanos

Department of Mechanical Engineering and Aeronautics, University of Patras, Patra, GR26500, Greece

ABSTRACT

One of the most frequently used techniques of structural health monitoring is the usage of piezoelectric materials as actuators or sensors. Piezoelectric wafers provide the ability of monitoring and self-excitation for detecting damage effects on structural vibration and wave propagation. In the area of delamination detection, attention is focused on the excitation and monitoring of symmetric and antisymmetric lamb waves, since they seem to be very promising to reveal the damage existence. The proposed paper will present layerwise mechanics and a finite element capable to describe the response of delaminated composite beams with piezoelectric actuators and sensors. A layerwise beam theory is formulated approximating the through-thickness and in-plane displacements and the electrical field as a continuous assembly of piecewise linear layerwise fields. The theory includes the ability to describe the discontinuities at the delamination region as additional degrees of freedom. The introduction of a variable transverse displacement field provides the capability to capture important antisymmetric Lamb modes at high-frequencies, and also other complex phenomena not captured by models assuming constant transverse displacement fields. Displacements and sensory voltage transient predictions are obtained capturing the high frequency wave propagation in delaminated composite beams. Further analysis of the transient numerical results provides dispersion curves illustrating the effect of the damage introduction on Lamb wave propagation.

1. INTRODUCTION

Composite materials seem to be attractive candidates to realize current and future trends imposed on aeronautical structures for weight reduction, improved performance, and operation in higher loads, higher temperatures and reduced manufacturing costs. However, the likelihood of internal voids and invisible damage initiation/propagation in composite materials during their service life remains high, thus fostering development of "intelligent" or "smart" composite structures with health monitoring capabilities. Among the many types of damage, attention is focused on the detection of delamination cracks, as they are usually induced through low-velocity impact, remain hidden, and can propagate in a catastrophic way. The development of modeling tools capable of capturing the effect of delaminations on the structural and material response remains an important issue of the problem, as such models may help to understand the sensitivity of various structural response parameters on present damage, may form the basis for damage detection and localization techniques and also for designing the SHM system. This paper presents the development of layerwise mechanics theory and a finite element for laminated beams with interlaminar cracks.

Early work in the area was focused on the effects of a single delamination on the natural frequencies of composite beams (Tracy and Pardoen,1989; Nagesh Babu and Hanagud,1990; Paolozzi and Peroni,1990; Shen and Grady,1992) and plates (Tenek et al.,1993; Rinderknecht and Kroplin,1995) using experimental results and simple analytical beam and plate models of the so-called "four-region" approach. Keilers and Chang (1995) presented experimental work for identifying a delamination in composite beams using built-in piezoelectric sensors. A

generalized composite beam model for predicting the effect of multiple delaminations on the modal damping and modal frequencies of composite laminates was reported together with experimental studies (Saravanos and Hopkins,1996), which treated the opening and sliding at the delamination interfaces as additional degrees of freedom. Barbero and Reddy (1991) used a layerwise laminate theory to describe plates with multiple delamination cracks between the layers. Di Sciuva and Librescu (2000) presented a geometrically non-linear theory of multilayered composite plates and shells with damaged interfaces, Luo and Hanagud (2000) presented a model for describing the static, modal and dynamic response of delaminated beams using a nonlinear approach based on piecewise linear spring models between the delaminated sublaminates, Thornburgh and Chattopadhyay (2001) used a higher order theory to model matrix cracking and delamination in laminated composite structures, Hu et al. (2002) analyzed the vibration response of delaminated composite beams using a higher-order finite element with C_0 type finite element, and Valdes and Soutis (1999) presented experimental work on the detection of delaminations in composite beams using piezoelectric actuator and sensor. Chrysochoidis and Saravanos (2004) investigated mainly experimentally, effects of delamination on the modal parameters and frequency response functions of artificially delaminated composite beams obtained via attached piezoceramic actuator and sensor pairs and demonstrated the potential of the latter compared to other traditional sensors. Chattopadhyay et al. (1999) studied the dynamics of delaminated composite plates with piezoelectric actuators using a third order shear theory and more recently (Chattopadhyay et al., 2004) reported a refined layerwise theory for the prediction of the vibration of delaminated plates considering the crack faces interface contact using a system of nonlinear springs.

Although very little work has been done in the area of Lamb modes and their usage as delamination indices. The present paper investigates the performance of a previously developed analytical model to predict propagation of Lamb waves. This model describes composite beams with various delamination cracks through the thickness assuming a variable normal displacements field and coupled electromechanical response. Also the present model has the ability to treat delamination relative movements as additional degrees of freedom of the beam. Performance of the developed model is investigated on predicted mode shapes, and its predictions are compared with an analytical Ritz solution. Additionally the transient response is predicted and its pseudo-Wigner-Ville distributions are presented for healthy and delaminated laminates.

2. THEORETICAL FORMULATION

Governing Material Equations. Each ply composite or piezoelectric is assumed to follow linear constitutive equations of piezoelectricity:

$$\begin{aligned} \sigma_i &= C_{ij}^E S_j - e_{ik} E_k \qquad i,j=1,\ldots,6 \\ D_m &= e_{mj} S_j + \varepsilon_{mk}^S E_k \qquad k,m=1,\ldots,3 \end{aligned} \tag{1}$$

σ_i and S_j are the mechanical stresses and engineering strains in vectorial notation; E_m is the electric field vector; D_m is the electric displacement vector; $C_{ij,}$ e_{lk} and ε_{mk} are the elastic stiffness; piezoelectric and electric permittivity tensors respectively. Superscripts E and S indicate constant electric field and strain conditions, respectively. The above equations encompass the behavior of an off-axis homogenized fibrous piezocomposite layer.

Equations of Motion. The variational statement of the equations of equilibrium for the piezoelectric structure is,

$$\begin{aligned} &\int_A -\delta H dA + \int_A \delta \underset{\sim}{u}(-\rho \ddot{\underset{\sim}{u}}) dA + \oint_{\Gamma_\tau} \delta \overline{\underset{\sim}{u}}^T \overline{\tau} d\Gamma + \\ &+ \oint_{\Gamma_D} \delta \overline{\varphi} \overline{D} d\Gamma = 0 \end{aligned} \tag{2}$$

where A is the x-z surface of the beam; H_L is the electric enthalpy of the piezoelectric laminate; $\overline{\tau}$ and $\overline{D}$ are, respectively, the surface tractions and charge, acting on the boundary surface Γ_τ, Γ_D; $\underset{\sim}{u} = \begin{Bmatrix} u \\ w \end{Bmatrix}$ is the displacement vector.

Kinematic Assumptions. A typical laminate is assumed to be subdivided into N discrete layers, where each discrete-layer may contain either a single ply, or a sub-laminate, or a sub-ply. The damage, consisting of either a single or multiple delamination cracks is considered to exist at the interfaces of two adjacent plies. Piecewise linear in-plane, transverse displacement and electric potential fields are assumed through the laminate thickness, which maintain continuity across the discrete layer boundaries, yet, allow for different slopes within each discrete layer, and admit sliding and opening across a delamination crack. In this manner, the displacement field (schematically shown in Figure 5) of the laminate, taking into account N_d delamination cracks takes the form:

$$u(x,z)=\sum_{i=1}^{N}\left(u^{i}(x)\psi_{1}^{i}(z_{i})+u^{i+1}(x)\psi_{2}^{i}(z_{i})\right)+ \\ +\sum_{k=1}^{Nd}\tilde{u}^{k}(x)\psi^{k}(z_{k})H(z-z_{k}) \tag{3}$$

$$w(x,z)=\sum_{i=1}^{N}\left(w^{i}(x)\psi_{1}^{i}(z_{i})+w^{i+1}(x)\psi_{2}^{i}(z_{i})\right) \\ +\sum_{k=1}^{Nd}\tilde{w}^{k}\psi^{k}(z_{k})H(z-z_{k}) \tag{4}$$

$$\varphi(x,z)=\Phi^{i}(x)\psi^{i}(z_{i})+\Phi^{i+1}(x)\psi^{i+1}(z_{i}) \tag{5}$$

where, superscripts i=1,...,N indicate the discrete layers, k=1,…,N^d the number of the delaminations through the thickness. At equations (3) and (4) terms u^i, u^{i+1} and w^i, w^{i+1} denote the axial and transverse displacements respectively at the interfaces of each discrete layer effectively describing the extension, rotation and through-thickness stretching, of the layer. Also $\tilde{u}^k$ and $\tilde{w}^k$ are the new degrees of freedom describing the sliding and opening across the faces of the k^{th} delamination (relative displacements). H is the Heaviside's step function and z_k is the distance of the k^{th} delamination from the mid-plane.

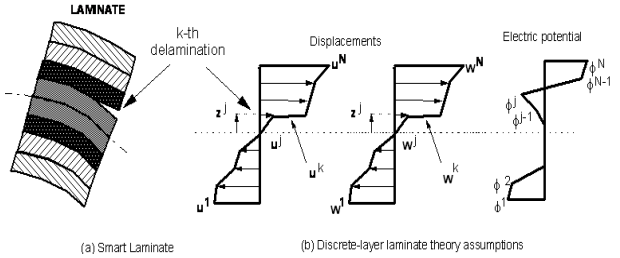

Figure 1. Illustration of the assumed displacement and electrical fields through the thickness of a delaminated composite laminate

Finally, Ψ^i and Ψ^k are the linear interpolation functions through the layer thickness and z_i is the thickness coordinates of layer i and z_k the thickness of the layer above the k^{th} crack. Also φ is the electric potential and Φ^i and Φ^{i+1} are the potentials at interfaces of each layer.

Generalized strain and electric field relations. The kinematic assumptions in eqs. (3-4) yield in each discrete layer an axial, transverse and shear strains S_1, S_3 and S_5 and an axial and transverse electrical field component of the form,

$$S_{1}=\sum_{i=1}^{N}\left(u_{,x}^{i}\psi_{1}^{i}+u_{,x}^{i+1}\psi_{2}^{i}\right)+\sum_{k=1}^{Nd}\tilde{u}_{,x}^{k}\psi^{k}H(z-z_{k}) \tag{6}$$

$$S_{3}=\sum_{i=1}^{N}\left(w^{i}\psi_{1,\zeta_{i}}^{i}\frac{2}{hi}+w^{i+1}\psi_{2,\zeta_{i}}^{i}\frac{2}{hi}\right)+ \\ +\sum_{k=1}^{Nd}\left(\tilde{w}^{k}\psi_{,\zeta_{i}}^{k}\frac{2}{hi}H(z-z_{k})+\hat{w}^{k}\psi^{k}\hat{\delta}(z-z_{k})\right) \tag{7}$$

$$S_{5}=\sum_{i=1}^{N}\left(w_{,x}^{i}\psi_{1}^{i}+w_{,x}^{i+1}\psi_{2}^{i}+\frac{2}{h_{i}}\left(u^{i}\psi_{1,\zeta_{i}}^{i}+u^{i+1}\psi_{2,\zeta_{i}}^{i}\right)\right)+ \\ +\sum_{k=1}^{Nd}\left[\left(\tilde{w}_{,x}^{k}\psi^{k}+\tilde{u}^{k}\psi_{,\zeta_{k}}^{k}\frac{2}{h_{k}}\right)H(z-z_{k})+\tilde{u}^{k}\psi^{k}\hat{\delta}(z-z_{k})\right] \tag{8}$$

$$E_{1}=\sum_{i=1}^{N}\left(-(\Phi_{,x}^{i}\Psi_{1}^{i}+\Phi_{,x}^{i+1}\Psi_{2}^{i+1})\right) \tag{9}$$

$$E_{3}=\sum_{i=1}^{N}\left(-(\Phi^{i}\Psi_{,\zeta_{k}}^{i}+\Phi^{i+1}\Psi_{,\zeta_{k}}^{i+1})\frac{2}{h_{k}}\right) \tag{10}$$

where $\hat{\delta}$ is the Dirac impulse function. In the above strain equations (6) to (8), $u^i_{,x}$, $u^{i+1}_{,x}$, $w^i_{,x}$, $w^{i+1}_{,x}$ represent S_1 and S_3 strain contributions, respectively, within each discrete layer of a healthy laminate, whereas, $u^k_{,x}$ and $w^k_{,x}$ expresses effect of the k^{th} delamination on the axial and transverse strains S_1 and S_3 above the crack. In the shear strain equation (8), the sum of the first two terms yields a constant shear strain term through the layer and the last two the effect of delamination. Equation (10) offers a constant variation in the electrical field in each discrete layer. The previous strain and electrical field equations were included into the variational form of motion equations, and the equivalent laminate stiffness and mass matrices were derived.

Analytical Solution (RITZ). The boundary conditions of a simply supported healthy beam are $w(0,z)=w(L,z)=0$ and $u(L/2,z)=0$. A fundamental set of mode shapes satisfying the boundary conditions is:

$$u(x,t)=U_{k}(t)\cdot\cos(ax) \\ w(x,t)=W_{k}(t)\cdot\sin(ax) \tag{11}$$

where $a=(k\pi)/L$. L is the beam length and k is the number of semi-wavelengths along the x direction of the respective mode indicated as mode k.

Finite Element Formulation. A 2 node beam finite element was formulated based on the previous laminate mechanics with linear shape functions N(x) used for the in plane, interlaminar displacements and electric potentials. In this manner, the local approximations of the generalized state variables in the element take the form:

$$\left\{u^i(x,t),\tilde{u}^k(x,t),w^i(x,t),\tilde{w}^k(x,t)\right\} =$$
$$= \sum_{i=1}^{L}\left\{u^{im}(t),\tilde{u}^{km}(t),w^{im}(t),\tilde{w}^{km}(t)\right\}N^i(x) \qquad (12)$$
$$\Phi^k(x) = \sum_{i=1}^{L}\Phi^{ki}N^i(x)$$

where i=1,...,N+1 and k=1,...,N^d (maximum number of delaminations that exist through the thickness of the element); L denotes the element length, for a 2-node L=2 beam element. Substituting the above equations into the governing equations of equilibrium which are expressed in variational form (2), the coupled piezoelectric system can be expressed in a discrete matrix form:

$$\begin{bmatrix}\left[M_{uu}\right] & 0\\ 0 & 0\end{bmatrix}\begin{Bmatrix}\{\ddot{u}\}\\ \{\varphi^S\}\end{Bmatrix}+\begin{bmatrix}\left[K_{uu}\right] & \left[K_{u\varphi}^{FF}\right]\\ \left[K_{\varphi u}^{FF}\right] & \left[K_{\varphi\varphi}^{FF}\right]\end{bmatrix}\begin{Bmatrix}\{\bar{u}\}\\ \{\varphi^F\}\end{Bmatrix} =$$
$$= \begin{Bmatrix}\{P\}-\left[K_{u\varphi}^{FA}\right]\{\varphi^A\}\\ \{Q^F\}-\left[K_{\varphi\varphi}^{FA}\right]\{\varphi^A\}\end{Bmatrix} \qquad (13)$$

Submatrices $\left[K_{uu}\right]$, $\left[K_{u\varphi}\right]$ and $\left[K_{\varphi\varphi}\right]$ indicate the total elastic, piezoelectric and permittivity matrices of the beam structure; $\left[M_{uu}\right]$ indicates the mass matrix; material, structural and delamination parameters are included in the previous sublaminates. Superscripts F and A indicate, respectively, sensory (free) and active (applied) electric potential components; {P} is the applied mechanical force vector and $\{Q^F\}$ is the applied electric charge at the sensors. The previously described electromechanical system using the Newmark time integration method is used to predict the time response of delaminated composite beams.

3 LAMB WAVES

Lamb waves apart from symmetric and antisymmetric forms, may vary according to the type of displacements these participating in the wave. Figure 2 illustrates the symmetric and antisymmetric types of elastic waves propagation representing the axial or normal displacements through the thickness of the elastic media. For the needs of the current work, the performance of the developed model in capturing all the types of Lamb modes will be investigated.

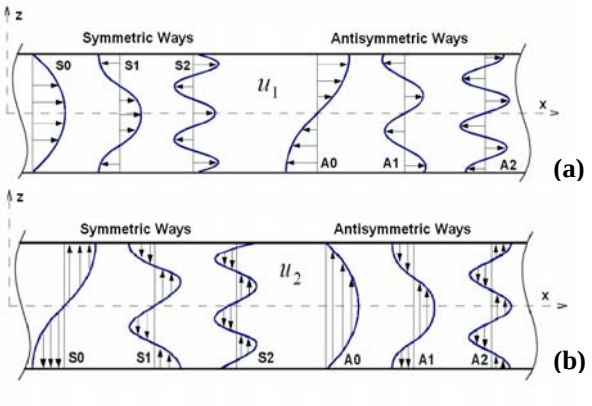

Figure 2. Symmetric and antisymmetric ways of wave propagation of (a) axial and (b) normal displacements

4. RESULTS AND DISCUSSION

4.1 Materials

This section presents numerical predictions of the analytical model described above. Predictions are for graphite/epoxy beams T300/934 having lamination $[0/90/45/-45]_s$, fiber volume ratios in the range of 0.57-0.63, nominal ply thicknesses 1.27mm, length 280mm and width 25mm. In some cases attached piezoceramic patches are considered on the beam surface. These patches are used either as actuators or sensors and have the characteristics of the PZ27 piezoceramics (Ferroperm). Material properties of the composite and the piezoceramics are illustrated in Table 1. Also the positions where the patches are attached on the beam are illustrated in Figure 8a. Additionally in some cases a delamination crack is modelled covering 5 or 10% of the total beam length. Configuration of the delaminated beam with piezoceramics is presented in Figure 10.

Table 1 Material properties

Property	***T300/934***	***Pz27 (Ferroperm)***
E_{11} (GPa)	127	58.82
E_{33} (GPa)	7.9	43.1
v_{13}	0.275	0.371
G_{13} (GPa)	3.4	22.98
d_{31} (m/V)	0	$-170\cdot10^{-12}$
d_{33} (m/V)	0	$425\cdot10^{-12}$
d_{15} (m/V)	0	$506\cdot10^{-12}$
ε_{31} (farad/m)	0	$15.94\cdot10^{-12}$
ε_{11} (farad/m)	0	$15.94\cdot10^{-12}$
ρ (kg/m^3)	1578	7700

4.2 Lamb mode shapes

Mode shapes of symmetric and antisymmetric through-thickness modes were predicted and identified for healthy and delaminated composite beams. All simulations refer to the carbon/epoxy composite specimens previously described.

4.2.1. Healthy beams.

In this case predictions were done in order to investigate the performance of our analytical model to predict all the types of Lamb modes described above. Additionally symmetric and antisymmetric ways of wave propagation are simulated using either Ritz or finite element solution offering the ability to validate the developed finite element model.

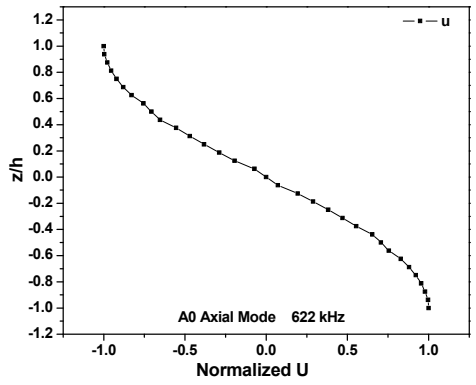

(a)

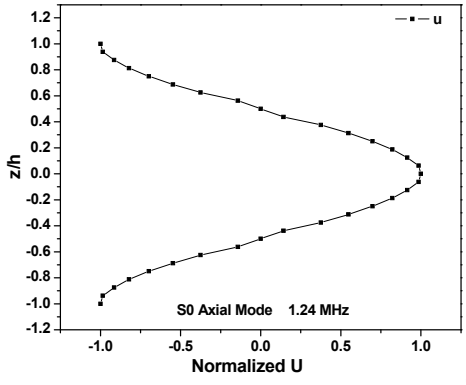

(b)

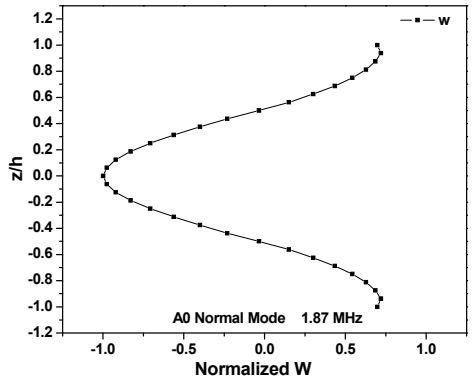

(c)

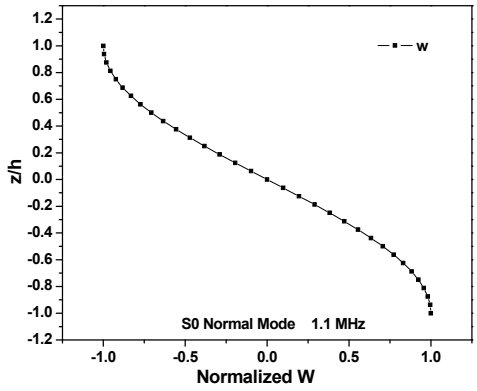

(d)

Figure 3 Elastic media Lamb modes. (a) Antisymmetric axial Ao; (b) Symmetric axial So; (c) Antisymmetric normal Ao; (d) Symmetric normal So modes

Predictions of the developed finite element offer similar distributions through the thickness. Additionally, Table 2 compares the predicted corresponding modal frequencies obtained via the Ritz and the FE solution. The small difference is owed to the utilization of reduced integration for some terms and full for the others. Despite these small differences, the performance of our analytical model to predict and simulate symmetric and antisymmetric mode shapes for healthy beams is illustrated.

Table 2 Comparison of modal frequencies between Ritz and FEM

	Ritz	**FEM**
Ao Axial	615 KHz	619 KHz
So Normal	1.11 MHz	1.12 MHz
So Axial	1.32 MHz	1.33 MHz
Ao Normal	1.89 MHz	2.23 MHz

4.2.2 Delaminated Composite Beams

So Symmetric Lamb modes of the normal displacements are additionally predicted for pristine and delaminated beams. This type of mode seems to be promising to reveal the delamination existence as it causes axial changes of the beam thickness. We selected two different sizes of delamination covering 5 and 10% of the

total beam length. Predictions were done under free-free supporting conditions and are illustrated at figures 4a to c.

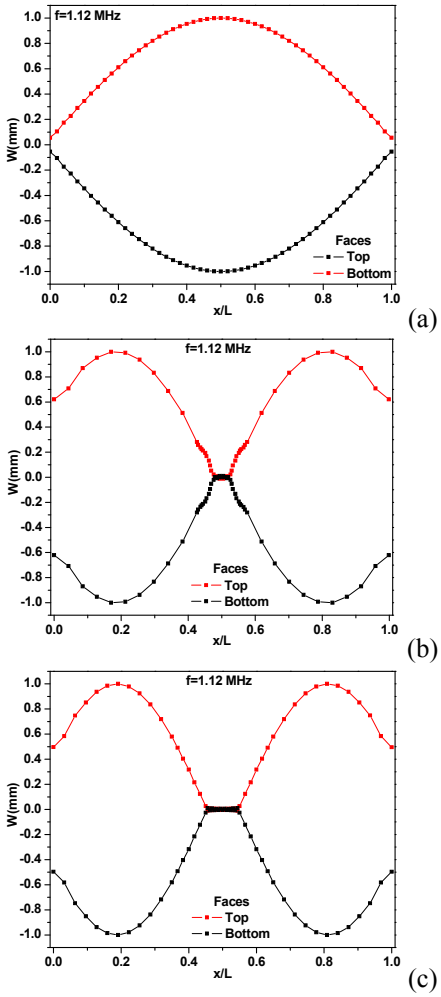

Figure 4 Lamb modes of unidirectional delaminated composite beams: (a) Pristine; (b) with 5% delamination; (c) with 10% delamination

Simulations of the normal symmetric mode present a drastic change at the predicted beam mode shape with the delamination introduction. It looks like the beam is separated into four different regions. Two regions at the top and bottom face of the crack, which remain still and two healthy regions at the left and right side of delamination. Additionally, the modal frequency remains the same with the healthy structure. This phenomenon is explained assuming that the modal frequencies of the Lamb modes depend only on the beam thickness and material properties. So for the regions at the two sides of the crack, which seem to be excited, the thickness is the same with this of the healthy laminate. On the other hand, due to the smaller thicknesses in the delaminated regions, the corresponding Lamb modal frequency is much higher, and they appear to remain still.

4.3 Time-Frequency Analysis of the Dispersion of Lamb Modes

4.3.1 Pseudo-Wigner-Ville Distributions

Transient response of healthy and delaminated composite beams is further simulated. Beams are excited either via a normal force or voltage at the piezoceramic actuator and the beam time response is predicted for both displacements and sensory voltage. Transient analysis results are further analyzed and pseudo-Wigner-Ville distributions (PWVD) are extracted. These distributions examine how the frequency content of a given signal changes as a function of time. An important advantage of the PWVD is the ability to analyze signals containing multiple propagation modes and/or reflections can be separated in the time-frequency space. Another advantage of these distributions is that they offer a first indication of the signal propagation velocity and time-of-flight between actuator and sensor. For the needs of this manuscript PWVD are generated using the Matlab time-frequency toolbox.

4.3.2 Lamb Modes

The performance of the PWVD to capture the dispersion of the Lamb modes is further investigated. Transient response of the healthy simply supported Carbon/Epoxy beam previously described is simulated. The beam is actuated with a normal Gaussian pulse force having the shape shown in Figure 5a, central frequency at 1 MHz and is applied at the position indicated in Figure 5b.

PWV distributions of the structural response under this actuation signal are shown in Figures 6a and b. Each one of these plots consists of three subplots. The top is the time response of the beam, the left presents the frequency content of the time response, and finally the contour plot shows the PWV distribution.

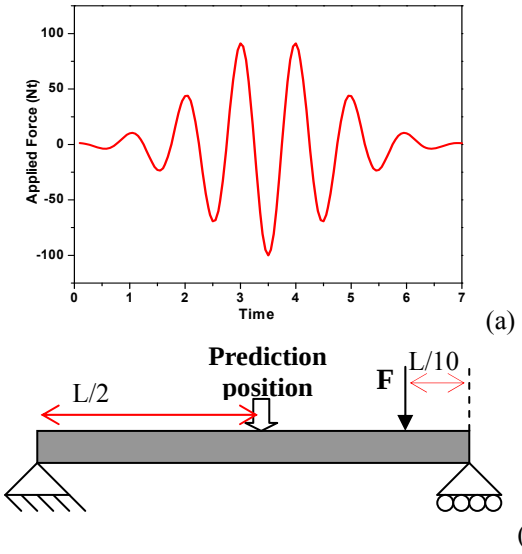

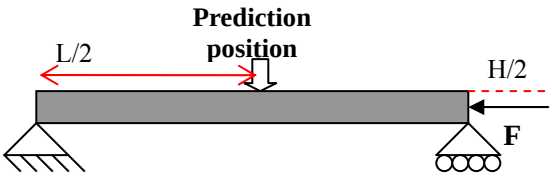

(c)

Figure 5. Simulation parameters. (a) Tone burst actuation signal; (b) Position of applied normal force and measurement; (c) Position of applied horizontal force

Figure 6a illustrates normal displacements at the top of the laminate and b the axial displacements measured at the same point at mid-thickness. Prediction position across the length is additionally indicated in Figure 5b. From these plots we can see that the So normal lamb mode who appears at 1.1 MHz is clearly excited and captured from both predictions with a bold horizontal line. Additionally at the second figure with the axial displacements the actuation signal is initially captured. In both cases when the structure is actuated under a normal force, a transverse wave is propagated and the captured signal has a significant time of flight and a signal with high duration dispersion.

As a next step, the simply supported beam is alternatively actuated under the same type of force pulse having central frequency 1.5MHz, but applied this time horizontally at the position shown at Figure 5c. Predictions are illustrated in Figures 7a and b. The first Figure, presenting normal displacement predictions, captures a mode with high duration at 1.1 MHz, which represents the previous So normal mode. Additionally a signal with smaller duration is captured approximately at 1.35 MHz, perhaps representing the So axial Lamb mode, who appears at this frequency as shown in Table 2. Our conclusion is enforced from Fig. 7b, showing the axial displacements, where a mode is captured at 1.35MHz having small duration and time of flight. This mode represents a longitudinal wave, which propagates faster and is probably the axial Lamb mode.

In general, the previous Figures, revealed the benefit of PWVD to analyse signals containing multiple propagation modes. It helps understanding the type of signal offering more information compared to the simple FFT plots illustrated at the left.

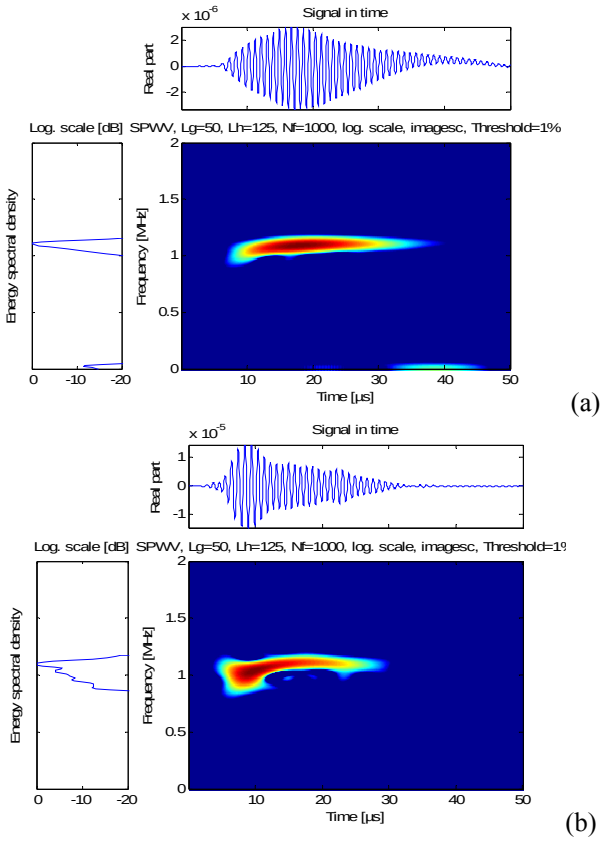

Figure 6. PWV distributions simulated for a normal force excitation: (a) transverse displacements; (b) axial displacements

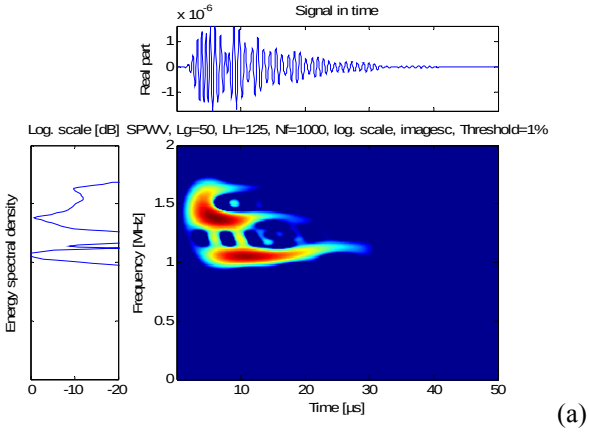

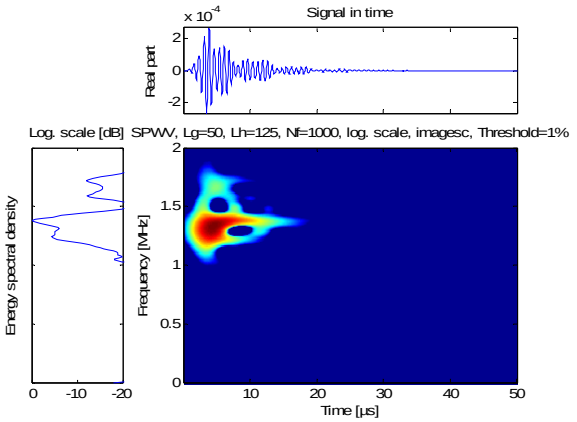

(b)

Figure 7. PWV distributions simulated for a horizontal force excitation: (a) transverse displacements; and (b) axial displacements

4.3.3 Healthy Beam with Active Piezosensor

A more realistic health monitoring system of a healthy Carbon/epoxy composite beam was further modelled with two piezoceramic patches on its surface. Using one of these piezoceramics as actuator and the other as sensor, the sensitivity of our model to predict lamb modes on the voltage and displacements time response is further investigated.

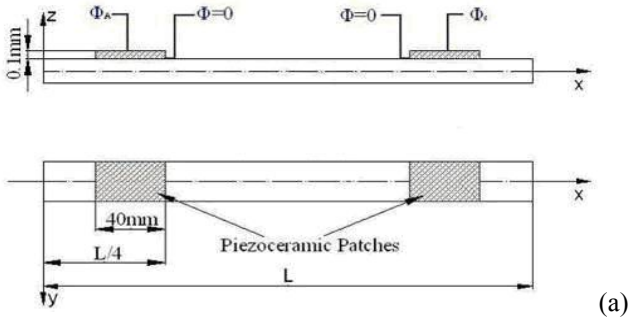

(a)

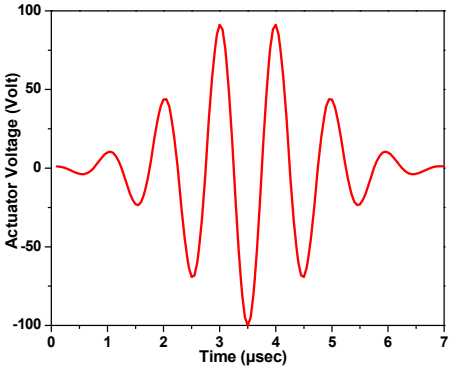

(b)

Figure 8. Setup of analytical simulation (a) beam with actuator and sensor patch and (b) Gaussian pulse actuation signal.

The position of the piezoceramics, as well as the applied Gaussian pulse voltage at the actuator, are illustrated in Figures 8a-b respectively. The central frequency of the actuation is 1MHZ like in the previous case, which is an actuation close to the So normal Lamb mode.The simulated electromechanical response is illustrated in Figures 9 a to c. Figs. 9a and 9b present the normal and axial displacements respectively at the top of the composite laminate under the piezoceramic sensor, and Fig. 9c the predicted sensory voltage. According to the previous predictions, we expect to capture a signal of 1.1 MHz in the normal displacements. Instead, the structure appears to be actuated at a frequency slightly lower than 1MHz. This is due to the locally changed structural thickness, which now appears increased due to the piezoceramic patch addition. Hence, the signal captured from the plot 9a is the So normal lamb mode of a thicker structure. This conclusion was also validated using modal analysis. Continuing, the axial displacements and the sensory voltages appear to have enough sensitivity to capture the dynamic characteristics of the simple composite laminate. In both cases, the simulations seem to capture the So normal lamb mode, who appears at 1.1 MHz. These results enforce the worthiness of the developed finite element and PWVD distributions in capture the Lamb wave propagation of a composite structure with active-sensory piezosystems. Additional numerical results, which are not shown due to space limitations, suggest that the performance of the sensor decreases with an increasing piezoceramic patch thickness. To avoid this adverse effect, we selected a really thin piezoceramic, 0.1mm thick.

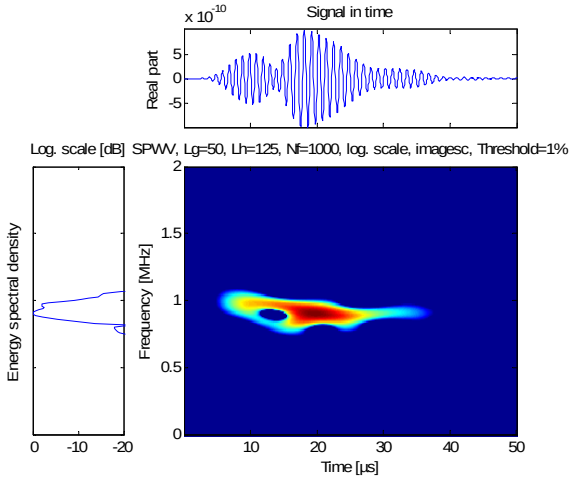

(a)

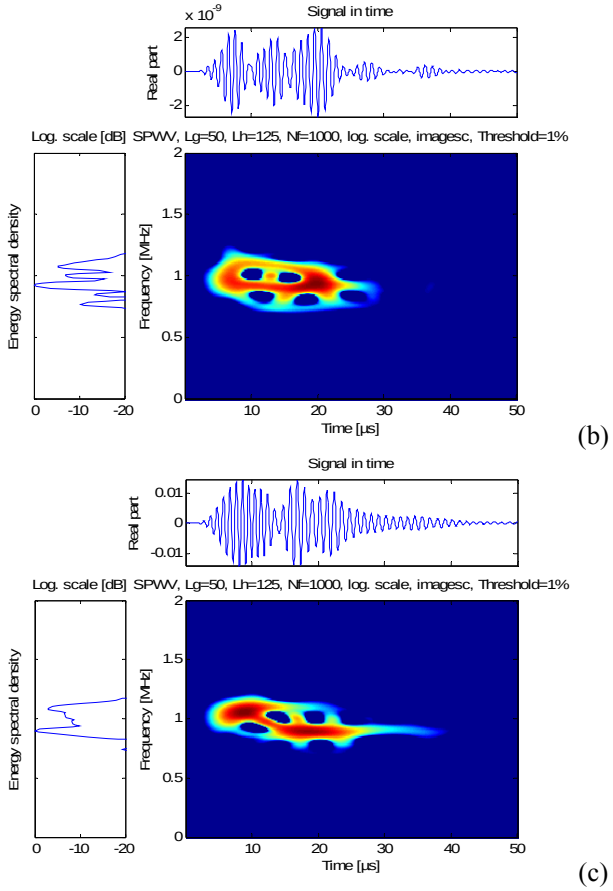

Figure 9. PWVD of the healthy active sensory beam: (a) normal displacements; (b) axial displacements; and (c) sensory voltage.

4.3.4 Delaminated Beam with Active Piezosensor

The FE model was further applied to investigate the effects of delamination on the response of composite beams. Thus a small delamination crack covering 5% of the total length was modeled at the middle of the composite beam, as shown in Figure10.

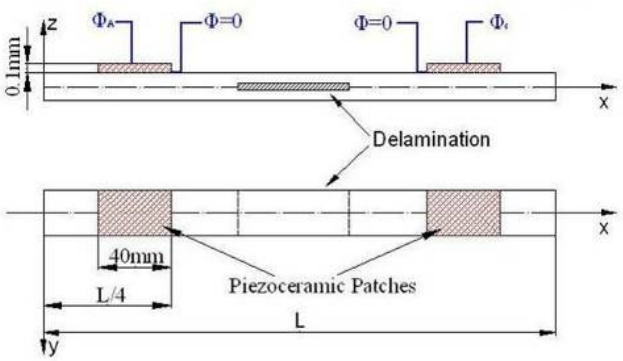

Figure 10. Delaminated composite beam with piezoceramic patches.

The applied signal at the piezoceramic actuator is the same as in the previous case (Figure 8b) of the healthy structure having a center frequency 1MHz. Predictions are illustrated in Figures 11a to c. These are the analogous predictions, as in the previous case of the healthy structure..

Comparing Figs. 9 and 11, the conclusions about the damage detection seem to be very promising. Due to the reasons mentioned above the predicted displacement and sensory voltage response are drastically affected by the delamination. Initially the duration of the signal dispersion is increased. Also there are changes at the shapes and the frequencies captured probably due to the independent vibration of the delamination crack. Assuming the very small size of the delamination, which covers only 5% of the model length, Lamb waves and PWVD provide a very promising and sensitive damage indicator.

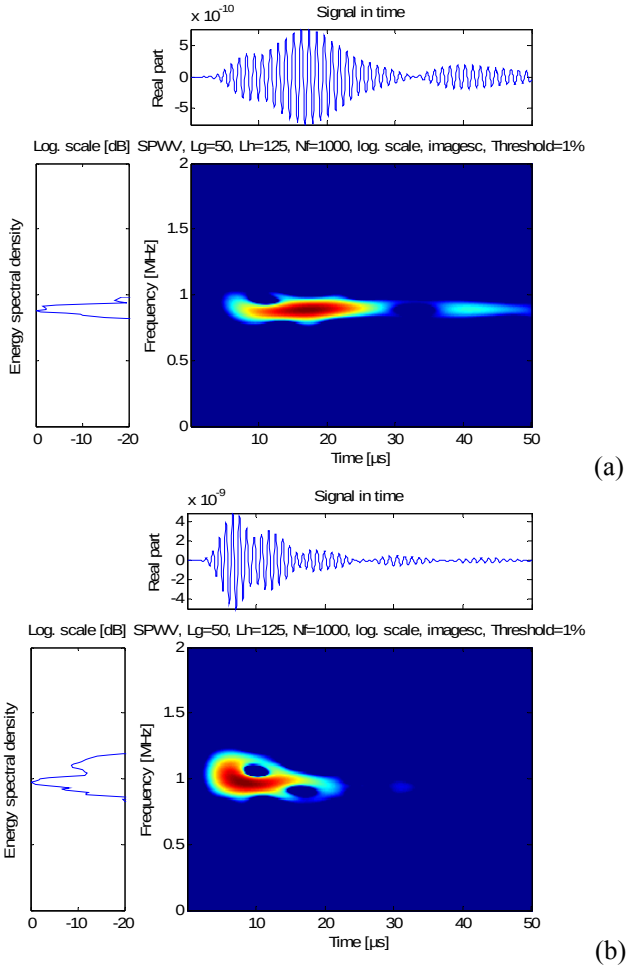

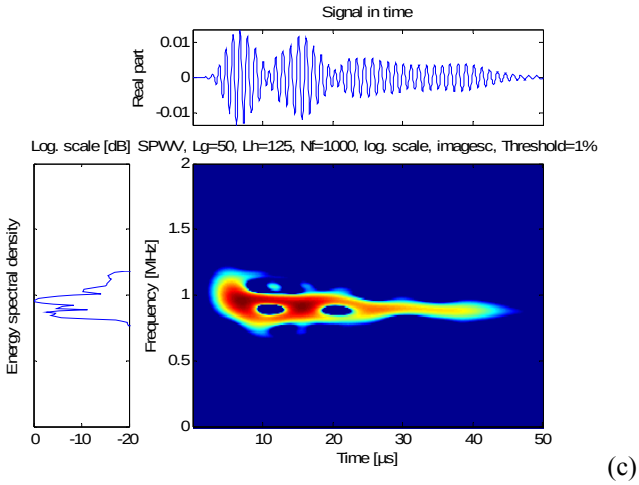

(c)

Figure 11. PWVD of the delaminated active sensory beam (a) normal displacements, (b) axial displacements and (c) sensory voltage.

5. CONCLUSIONS

A linear layerwise beam finite element and analytical (RITZ) model was developed having the ability to describe the electromechanical response of composite beams with multiple delamination cracks. This model treats delamination relative movements, opening and sliding, as additional degrees of freedom. The main advantage of the developed model is the ability to describe variations at the normal displacements using a piecewise linear transverse displacements field.

Performance of the developed formulation was further investigated to predict various types of lamb modes on the modal and transient beam response. Initially, the accuracy of the developed beam finite element was examined via correlations with a Ritz solution. Comparison of modal frequencies presented a quite good agreement and the ability of the developed linear layerwise theory to describe all the types of lamb modes was demonstrated. Additionally the So normal lamb mode shapes were predicted for healthy and delaminated beams. Finally the importance of structure's thickness on the predicted lamb modes shapes was mentioned.

Time response of the developed finite element with normal displacement variations was additionally simulated for the healthy structure. Predictions were presented for excitation frequencies above 1MHz and their aim was to capture pure composite beam lamb modes. Pseudo-Wigner Ville-distributions were produced for the normal and axial displacements, and the sensory voltage.

Three cases were simulated. The first two addressed healthy beam structures, the first actuated via an ideal applied force, the second via a piezoceramic actuator. In both cases the ability of the present model to capture the lamb modes was demonstrated. This sensitivity of the system was reduced when piezoceramic patches were placed on the specimen surface. however the sensor voltage illustrated ability to detect the structural Lamb modes.

The third case was a beam with a delamination crack covering 5% of the total length with an active piezosensor. In this case, the effect of damage was found on the duration of the simulated signal dispersion. The introduction of this small size crack has shown high sensitivity of the response predictions and makes Lamb modes at these frequency levels promising damage indicators. Future work will focus on comparisons with experimental measurements, which will enforce our conclusions.

ACKNOWLEDGMENTS

This work was funded by the European Social Fund (ESF), Operational Program for Educational and Vocational Training II under the Graduate Research Program HERAKLETOS. This funding is gratefully acknowledged by the authors.

REFERENCES

References

1. Tracy, J.J. and Pardoen, G.C., 1989. "Effect of delamination on the natural frequencies of composite laminates." *Journal of Composite Materials* 23 pp.1200-1215.

2. Nagesh Babu, G.L. and Hanagud, S., 1990. "Delaminations in smart composite structures: a parametric study on vibrations." *In: Proceedings of the 31st AIAA/ASME/ASCE/AHS/ASC SDM Conference*, AIAA paper 90-1173-CP, 2417-2426.

3. Paolozzi, A. and Peroni, I., 1990. "Detection of debonding damage in a composite plate through natural frequency variations." *Journal of Reinforced Plastics and Composites* 9 pp.369-389.

4. Shen, M.H.H. and Grady, I., 1992. "Free vibrations of delaminated beams." *AIAA Journal* 30 (5) 1361-1370.

5. Tenek, L.H., Henneke, E.G. and Gunzburger, M.D., 1993. "Vibration of delaminated composite plates and some applications to non-destructive testing." *Composite Structures* 23 pp. 253-262.

6. Rinderknecht, S. and Kroplin, B., 1995. "A finite element model for delamination in composite plates." *Mechanics of Composite Material and Structures* 2 pp. 19-47.

7. Keilers, C.H. and Chang, F.K., 1995. "Identifying delamination in composite beams using built-in piezoelectrics .1. Experiments and analysis." *Journal of Intelligent Material Systems and Structures* 6 (5) 649-663.

8. Saravanos D.A. and Hopkins, D.A., 1996. “Effects of delaminations on the damped dynamic characteristics of composite laminates: Analysis and experiments.” *Journal of Sound and Vibration* 192 (5) 977-993.
9. Barbero E.J and Reddy, J.N., 2001. “Modeling of delamination in composite laminates using a layerwise plate theory.” *International Journal of Solids and Structures* 28 (3) 373-388.
10. Di Sciuva, M. and Librescu, L., 2000. “A dynamic nonlinear model of multilayered composite shells featuring damage interfaces.” *In Proceedings of the 41st AIAA/ASME/ASCE/ AHS/ASC SDM*, AIAA-2000-1384, Atlanta , GA, April 3-6
11. Luo, H. and Hanagud, S., 2000. “Dynamics of delaminated beams.” *International Journal of Solids and Structures* 37 pp. 1501-1519.
12. Thornburgh, R. and Chattopadhyay, A., 2001. “Unified approach to modeling matrix cracking and delamination in laminated composite structures.” *AIAA Journal* 39 (1) 153-160.
13. Hu, N., Fukunaga, H., Kameyama, M., Aramaki, Y. and Chang, F.K., 2002. “Vibration analysis of delaminated composite beams and plates using a higher-order finite element.” *International Journal of Mechanical Science* 44 (7) 1479-1503
14. Diaz Valdes, S.H. and Soutis, C. 1999. “Delamination Detection in Composite Laminates from Variation of their Modal Characteristics.” *Journal of Sound and Vibration*, 228(1), pp. 1-9.
15. Chrysochoidis, N.A. and Saravanos, D.A., 2004. “Assessing the effects of delamination on the damped dynamic response of composite beams with piezoelectric actuators and sensors.” *Smart materials and Structures* 13 (4) 733-742
16. Chattopadhyay, A., Gu, H. and Dragomir-Daescu, D., 1999. “Dynamics of Delaminated Composite Plates with Piezoelectric Actuators.” *AIAA Journal* 37 (2) pp.248-254
17. Chattopadhyay, A., Kim, H.S. and Ghoshal, A., 2004. “Non-linear vibration analysis of smart composite structures with discrete delamination using a refined layerwise theory.” *Journal of Sound and vibration* 273 (1-2) 387-407